Voronoi Cells of Singular Points on Real Plane Curves

Boris Shapiro

May 30, 2026

Abstract

We study Voronoi cells attached to singular points of real plane algebraic curves. The general algebraic theory of Voronoi cells of varieties, developed by Cifuentes–Ranestad–Sturmfels–Weinstein, treats smooth points and places the cell in the corresponding normal space. For a smooth point of a plane curve this gives a one-dimensional normal-line cell. We focus on what changes at a real singular point. The local cell may have non-empty interior in the ambient plane. We give a criterion for this phenomenon in terms of the polar cone of the real semi-tangent cone, construct its boundary as an envelope of perpendicular bisectors between the singular point and nearby real branches, and work out ordinary cusps, higher cusps, nodes, tacnodes and isolated real points. We also restructure the global part around the classical symmetry set: the algebraic curve of centers having at least two normal segments to the original curve of equal length. Its nearest-point part is the medial axis or jump locus; singularities add singular–smooth components. Brandt–Weinstein's algebraic study of plane-curve Voronoi cells, medial axes, evolutes, bottlenecks and reach supplies the smooth background, while the new contribution is the semi-tangent-cone correction at singular sites. The cusp $y^2 + x^3 = 0$ gives a basic two-dimensional singular Voronoi cell bounded by

$$X = \frac{t^2 + 3t^4}{2}, \qquad Y = t + 2t^3.$$

1 Introduction

Let $C \subset \mathbb{R}^2$ be a real algebraic curve and let $p \in C$. The Voronoi cell of p, with respect to the continuum of sites C, is

$$\mathcal{V}_C(p) = \{z \in \mathbb{R}^2 : |z - p| \le |z - q| \text{ for every } q \in C\}.$$

For a finite set of sites this is the usual Voronoi cell. For a curve one obtains a continuum version of the same construction. The general algebraic theory of Voronoi cells of varieties was developed in [7]; in particular, Voronoi cells of real algebraic varieties are convex semialgebraic sets in normal spaces. The special case of plane curves, including connections with medial axes, curvature, evolutes, bottlenecks and reach, was studied by Brandt and Weinstein [4]. Classical background includes Blum's medial axis and grassfire picture [3], symmetry sets of plane curves [5, 8], and the singularity theory of caustics and wave fronts [1, 2, 6].

Let us spell out the precise relation with these two recent papers. In [7], for a smooth point y of a real algebraic variety $X \subset \mathbb{R}^n$, the Voronoi cell $\mathrm{Vor}_X(y)$ is a convex semialgebraic subset of the Euclidean normal space $N_X(y)$, and the algebraic boundary is computed by a critical ideal obtained from the normal bundle and an equidistance equation. For a smooth point of a plane curve this immediately implies that the cell is contained in a line. In [4], this smooth plane-curve picture is developed in detail: Voronoi and Delaunay cells of plane curves are related to finite samples, and the medial axis, evolute, bottlenecks and reach are described algebraically. The present paper should be read as a small complement to these works. We keep their Voronoi viewpoint but ask what remains meaningful when the distinguished point of the curve is singular. Since the ordinary tangent space and normal space are no longer available at a singularity, the substitute used here is the polar of the real semi-tangent cone.

Department of Mathematics, Stockholm University, SE-106 91 Stockholm, Sweden. Email address: shapiro@math.su.se.
Keywords. Voronoi cells; real algebraic curves; plane curve singularities; semi-tangent cone; medial axis; symmetry set; evolute; wave front; cut locus.
2020 Mathematics Subject Classification. Primary 14P25, 14H20; Secondary 53A04, 58K05, 68U05.

A second point of terminology is important. The locus of centers having two distinct normal segments to a smooth curve with the same length is not a new curve: it is the classical *symmetry set* of Bruce–Giblin–Gibson, also called the Maxwell set of the squared-distance family. Its nearest-point part is the medial axis or cut locus. The ordinary evolute is the caustic or focal part, where one critical point of the squared distance degenerates. Thus the global discriminant of the squared-distance family is naturally decomposed into a Maxwell/symmetry part and a caustic/evolute part. This distinction is useful because the Euclidean distance discriminant in the algebraic ED-degree literature is usually the caustic/branch-locus object, while the codimension-one boundary of Voronoi chambers is the nearest-point part of the symmetry set.

Our main point is local but has a global consequence. For a smooth point $p \in C$, the cell lies in the normal line to the curve, until it is cut by a focal point, a symmetry-set point, or another global obstruction. At a singular point this normal-line picture is no longer adequate: a singular point may have a genuinely two-dimensional Voronoi cell. Its boundary is not, in general, the ordinary evolute; it is a singular bisector envelope obtained from the competition between the singular point and nearby smooth points.

The simplest example is the real cusp

$$C : y^2 + x^3 = 0, \qquad \gamma(t) = (-t^2, t^3).$$

The Voronoi cell of the cusp point at the origin is the region

$$X \geq \sup_{t \in \mathbb{R}} \left(Yt - \frac{t^2 + t^4}{2} \right),$$

whose boundary is

$$X = \frac{t^2 + 3t^4}{2}, \qquad Y = t + 2t^3.$$

This boundary is not the ordinary evolute of the cusp. It is the envelope of perpendicular bisectors of the chords joining the singular point to nearby smooth points of the curve. We call such an envelope a *singular Voronoi caustic*.

The elementary observation on which the paper rests is that the existence of a two-dimensional singular Voronoi cell is already visible from the real tangent directions of arcs approaching the singular point. The correct first-order object is not only the unoriented tangent cone, but the *semi-tangent cone*, keeping track of one-sided real directions. For instance, the cusp $(-t^2, t^3)$ approaches the origin with leading direction $(-1, 0)$, not with both directions of the x-axis. This is the point at which the discussion departs from the smooth normal-space formalism of [7] and from the smooth plane-curve metric features of [4].

Main local message

After translating a singular point to the origin, let $\mathcal{T}_0^+ C$ denote the closed cone generated by all leading vectors of real analytic arcs in C approaching the origin. Its polar cone is

$$(\mathcal{T}_0^+ C)^\circ = \{z \in \mathbb{R}^2 : \langle z, v \rangle \leq 0 \text{ for all } v \in \mathcal{T}_0^+ C\}.$$

Then, locally,

$$\boxed{\mathcal{V}_C(0) \text{ has non-empty interior near } 0 \quad \Longleftrightarrow \quad (\mathcal{T}_0^+ C)^\circ \text{ has non-empty interior.}}$$

This gives a practical classification criterion. Cusps with even leading exponent can produce two-dimensional cells. Ordinary real nodes, ordinary multiple points with genuine two-sided branches, and tacnodes with two opposite semi-tangent directions do not. Isolated real points produce locally full-dimensional cells.

2 Voronoi cells as intersections of half-planes

We shall work locally near a singular point. After translation we assume that the point is the origin. Let $(C, 0)$ be a real analytic plane curve germ. For a small neighborhood U of the origin define the local cell

$$\mathcal{V}_{C \cap U}(0) = \{z \in \mathbb{R}^2 : |z| \leq |z - q| \text{ for all } q \in C \cap U\}.$$

The global cell $\mathcal{V}_C(0)$ is obtained by adding inequalities coming from the rest of the curve.

The next observation is the same elementary inequality underlying the convexity of Voronoi cells in the general theory of [7]. We record it because at a singular point it remains valid even though there is no ordinary normal space.

Lemma 2.1 (Basic half-plane inequality)**.** *Let $q \in \mathbb{R}^2$. A point $z \in \mathbb{R}^2$ is at least as close to 0 as to q if and only if*

$$2\langle z, q\rangle \leq |q|^2.$$

Consequently

$$\mathcal{V}_C(0) = \bigcap_{q \in C} \{z : 2\langle z, q\rangle \leq |q|^2\}.$$

In particular, every Voronoi cell of a point on a curve is closed and convex.

Proof. The inequality $|z|^2 \leq |z - q|^2$ is equivalent to

$$|z|^2 \leq |z|^2 - 2\langle z, q\rangle + |q|^2,$$

which is precisely $2\langle z, q\rangle \leq |q|^2$. □

This elementary observation is useful because it reduces the local singular problem to the asymptotics of a family of linear inequalities.

3 Semi-tangent cones and the two-dimensionality criterion

Definition 3.1. *The* real semi-tangent cone *of $(C, 0)$, denoted $\mathcal{T}_0^+C$, is the closed convex cone generated by all non-zero vectors $v \in \mathbb{R}^2$ for which there exists a real analytic arc $\gamma(s) \in C$, $s > 0$, with $\gamma(0) = 0$ and*

$$\gamma(s) = s^m v + O(s^{m+1})$$

for some integer $m \geq 1$. Its polar cone is

$$(\mathcal{T}_0^+C)^\circ = \{z \in \mathbb{R}^2 : \langle z, v\rangle \leq 0 \text{ for all } v \in \mathcal{T}_0^+C\}.$$

The use of a semi-tangent cone rather than the usual tangent cone is essential. The usual tangent cone of a cuspidal branch often records only a line, whereas the Voronoi inequality sees the side from which the branch approaches the singular point.

Theorem 3.2 (Local two-dimensionality criterion)**.** *Let $(C, 0)$ be a real analytic plane curve germ. Then the local Voronoi cell $\mathcal{V}_{C\cap U}(0)$, for sufficiently small U, has non-empty interior near the origin if and only if the polar cone $(\mathcal{T}_0^+C)^\circ$ has non-empty interior. More precisely:*

(i) *the tangent cone at the origin of $\mathcal{V}_{C\cap U}(0)$ is contained in $(\mathcal{T}_0^+C)^\circ$;*

(ii) *every ray contained in the interior of $(\mathcal{T}_0^+C)^\circ$ is contained in the tangent cone of $\mathcal{V}_{C\cap U}(0)$.*

Proof. Let $z_s \in \mathcal{V}_{C\cap U}(0)$ be an arc with $z_s = sw + o(s)$. Let $v \in \mathcal{T}_0^+C$. By definition there is an arc $q(t) = t^m v + O(t^{m+1})$ in C. Lemma 2.1 gives

$$2\langle z_s, q(t)\rangle \leq |q(t)|^2.$$

For fixed $s > 0$, divide by t^m and let $t \to 0^+$. We get $\langle z_s, v\rangle \leq 0$. Dividing by s and letting $s \to 0^+$, we obtain $\langle w, v\rangle \leq 0$. Hence $w \in (\mathcal{T}_0^+C)^\circ$. This proves (i).

Conversely, suppose $w \in \mathrm{int}((\mathcal{T}_0^+C)^\circ)$. The set of normalized semi-tangent directions is compact, hence there exists $\eta > 0$ such that

$$\langle w, v\rangle \leq -\eta|v|$$

for every semi-tangent vector v. The same strict inequality persists in a small cone K around w. Since a real analytic plane curve has only finitely many local branches, every local point $q \in C \cap U$ has leading direction in the semi-tangent cone. Shrinking U if necessary, we obtain

$$\langle z, q \rangle \leq 0$$

for all sufficiently small $z \in K$ and all $q \in C \cap U$. Therefore Lemma 2.1 gives $2\langle z, q\rangle \leq |q|^2$, so $z \in \mathcal{V}_{C\cap U}(0)$. This proves (ii). $\square$

Corollary 3.3. *Assume that 0 is an isolated point of $C \setminus (C \cap U)$, i.e. no other part of the curve accumulates at 0. If $(\mathcal{T}_0^+ C)^\circ$ has non-empty interior, then the global Voronoi cell $\mathcal{V}_C(0)$ contains a small sector with vertex at the origin. If $(\mathcal{T}_0^+ C)^\circ$ has empty interior, then no two-dimensional sector based at the origin can be contained in $\mathcal{V}_C(0)$.*

Proof. The local statement follows from Theorem 3.2. Points of $C \setminus U$ have distance bounded away from 0, so their inequalities are automatically satisfied by sufficiently small z in the local sector. The obstruction statement follows from part (i) of the theorem. $\square$

Remark 3.4. *The theorem is intentionally local. Globally, distant pieces of the same algebraic curve may cut off the sector or truncate it. The singularity determines the germ of the cell at the singular point, while the global curve determines its final convex shape.*

4 Consequences for common real singularities

The criterion gives an immediate classification for many simple singularities.

Proposition 4.1 (Smooth points do not contribute two-dimensional cells)**.** *Let p be a smooth point of a real analytic curve. Then the local Voronoi cell $\mathcal{V}_C(p)$ is contained in the normal line to C at p. Along this normal line, the local focal endpoint is the corresponding center of curvature, i.e. the point of the evolute lying on the normal.*

Proof. Translate p to 0. A local parametrization has the form $q(t) = t\tau + O(t^2)$, where τ is the tangent vector and both positive and negative values of t occur. The inequality $2\langle z, q(t)\rangle \leq |q(t)|^2$, divided by t and evaluated for $t \to 0^+$ and $t \to 0^-$, gives $\langle z, \tau\rangle = 0$. Thus z lies on the normal line. The usual second-order expansion in Frenet coordinates gives the focal endpoint at distance $1/\kappa$ in the curvature-normal direction. This is the ordinary center of curvature. $\square$

Proposition 4.2 (Branches with odd leading exponent)**.** *Let $(C, 0)$ have a real branch with parametrization*

$$\gamma(t) = at^m + O(t^{m+1}), \qquad a \neq 0,$$

where t takes both positive and negative values and m is odd. Then $\mathcal{T}_0^+ C$ contains both a and $-a$, so the polar cone is contained in the line $a^\perp$. In particular, this branch by itself prevents a two-dimensional local Voronoi cell.

Proof. For $t \to 0^+$ the leading vector is a, while for $t \to 0^-$ the leading vector is $-a$. Any vector in the polar cone must have non-positive scalar product with both a and $-a$, hence must be orthogonal to a. $\square$

Proposition 4.3 (Even cuspidal branches)**.** *Let $(C, 0)$ have one real branch with parametrization*

$$\gamma(t) = at^{2k} + O(t^{2k+1}), \qquad a \neq 0,$$

where both signs of t occur. If no other branch contributes the opposite leading direction, then the polar cone has non-empty interior. Hence the singular point has a two-dimensional local Voronoi cell.

Proof. Both halves of the parametrization have the same leading vector a. The first-order polar condition is the half-plane $\langle z, a\rangle \leq 0$. If no other branch contributes directions whose cone fills a line through a or surrounds the origin, this polar remains two-dimensional. Theorem 3.2 applies. $\square$

Corollary 4.4 (Ordinary cusps have two-dimensional cells)**.** *The ordinary cusp $y^2 = x^3$ or $y^2 + x^3 = 0$, at its cusp point, has a two-dimensional local Voronoi cell. More generally, a unibranch real cusp whose first non-zero parametrized term has even order has a two-dimensional local Voronoi cell, unless other local branches destroy the polar sector.*

Proposition 4.5 (Ordinary nodes and ordinary multiple points)**.** *Let $(C, 0)$ be an ordinary real multiple point whose local branches are smooth and real. Then the Voronoi cell of the singular point has no two-dimensional local sector. In particular, ordinary real nodes do not have two-dimensional singular Voronoi cells.*

Proof. Each smooth branch contributes two opposite semi-tangent directions. Already one such branch forces the polar cone to lie in the normal line to that branch. If there are two transverse branches, as in an ordinary node, the intersection of the two corresponding normal lines is $\{0\}$. Thus the polar cone has empty interior, and Theorem 3.2 applies. □

Proposition 4.6 (Tacnodes)**.** *Consider the standard tacnode*

$$y^2 = x^4,$$

with local branches $y = x^2$ and $y = -x^2$. The singular point has no two-dimensional local Voronoi cell.

Proof. The two branches may be parametrized as

$$\gamma_1(t) = (t, t^2), \qquad \gamma_2(t) = (t, -t^2).$$

For each branch, the leading term is $(t, 0)$, so both directions $(1, 0)$ and $(-1, 0)$ occur. The polar cone is therefore contained in the vertical line. Hence it has empty interior, and Theorem 3.2 gives the claim. □

Proposition 4.7 (Isolated real points)**.** *Suppose that $0 \in C(\mathbb{R})$ is an isolated real point of the real curve. Then for sufficiently small $\epsilon > 0$, the disk $|z| < \epsilon$ is contained in the local Voronoi cell of 0. Thus an isolated real point has a locally two-dimensional Voronoi cell, indeed a full neighborhood.*

Proof. If 0 is isolated in $C(\mathbb{R})$, then for sufficiently small U one has $C(\mathbb{R}) \cap U = \{0\}$. There are no local inequalities other than the trivial one. Hence every sufficiently small point z belongs to $\mathcal{V}_{C\cap U}(0)$. Global inequalities from points outside U are again harmless for z sufficiently close to 0. □

5 The bisector-envelope construction

The tangent cone criterion detects whether a two-dimensional cell exists, but it does not describe the curved boundary. The boundary is obtained effectively from a family of perpendicular bisectors.

Let $p = 0$ and let $\gamma(t)$ be a local real branch. The bisector between 0 and $\gamma(t)$ is

$$|z|^2 = |z - \gamma(t)|^2,$$

or equivalently

$$2\langle z, \gamma(t)\rangle = |\gamma(t)|^2.$$

Writing $z = (X, Y)$, this is a one-parameter family of lines

$$B(X, Y, t) = 0.$$

The envelope is obtained from

$$B(X, Y, t) = 0, \qquad \frac{\partial B}{\partial t}(X, Y, t) = 0.$$

For several branches one takes the corresponding envelopes and then keeps only those pieces which bound the intersection of all half-plane inequalities.

Definition 5.1. *A* singular Voronoi caustic *of $(C, 0)$ is a local component of the envelope of the perpendicular bisectors between 0 and nearby smooth points of C which appears in the boundary of $\mathcal{V}_C(0)$.*

This object is analogous to an evolute, but it is not the ordinary evolute. The ordinary evolute is the envelope of normals at smooth points. The singular Voronoi caustic is the envelope of bisectors between a fixed singular point and moving smooth points.

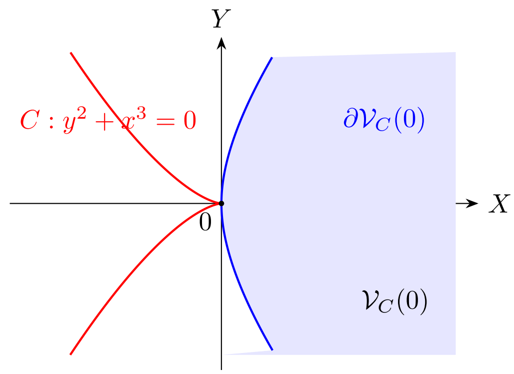

Figure 1: The cusp $y^2+x^3=0$ and the two-dimensional Voronoi cell of its singular point. The blue boundary is the singular Voronoi caustic.

6 Examples

6.1 The ordinary cusp

Consider

$$C : y^2 + x^3 = 0, \qquad \gamma(t) = (-t^2, t^3).$$

Let $z = (X, Y)$. The condition that z is closer to the origin than to $\gamma(t)$ is

$$X^2 + Y^2 \leq (X + t^2)^2 + (Y - t^3)^2.$$

After cancellation,

$$0 \leq 2Xt^2 - 2Yt^3 + t^4 + t^6.$$

For $t \neq 0$, division by t^2 gives

$$2X \geq 2Yt - t^2 - t^4.$$

Therefore

$$\mathcal{V}_C(0) = \left\{ (X, Y) : X \geq \sup_{t\in\mathbb{R}} \left(Yt - \frac{t^2 + t^4}{2} \right) \right\}.$$

The boundary is obtained by maximizing the right-hand side. The critical point satisfies

$$Y = t + 2t^3.$$

Substitution gives

$$X = Yt - \frac{t^2 + t^4}{2} = \frac{t^2 + 3t^4}{2}.$$

Thus

$$\boxed{\partial\mathcal{V}_C(0) : X = \frac{t^2 + 3t^4}{2}, \qquad Y = t + 2t^3.}$$

The cell is the region to the right of this curve. Near the origin,

$$X = \frac{Y^2}{2} + O(Y^4).$$

6.2 Higher cusps

Consider a branch

$$\gamma(t) = (-t^{2k}, t^{2k+1}), \qquad k \geq 1.$$

Then

$$|\gamma(t)|^2 = t^{4k} + t^{4k+2}.$$

The bisector inequality is

$$2(-Xt^{2k} + Yt^{2k+1}) \leq t^{4k} + t^{4k+2}.$$

Dividing by t^{2k} gives

$$X \geq Yt - \frac{t^{2k} + t^{2k+2}}{2}.$$

The boundary is the Legendre-type envelope of

$$Yt - \frac{t^{2k} + t^{2k+2}}{2}.$$

The critical equation is

$$Y = kt^{2k-1} + (k+1)t^{2k+1},$$

and therefore

$$X = Yt - \frac{t^{2k} + t^{2k+2}}{2} = \left(k - \frac{1}{2}\right) t^{2k} + \left(k + \frac{1}{2}\right) t^{2k+2}.$$

Thus the singular Voronoi caustic is

$$\boxed{X = \frac{2k-1}{2} t^{2k} + \frac{2k+1}{2} t^{2k+2}, \qquad Y = kt^{2k-1} + (k+1)t^{2k+1}.}$$

For $k = 1$ this is exactly the ordinary cusp computed above.

6.3 The ramphoid cusp

The real ramphoid cusp

$$y^2 = x^5, \qquad \gamma(t) = (t^2, t^5),$$

has leading direction $(1, 0)$, hence its singular Voronoi cell opens to the left. The bisector inequality is

$$2(Xt^2 + Yt^5) \leq t^4 + t^{10}.$$

For $t \neq 0$, after division by t^2,

$$X \leq -Yt^3 + \frac{t^2 + t^8}{2}.$$

The boundary is obtained from

$$X = -Yt^3 + \frac{t^2 + t^8}{2}.$$

Differentiating gives

$$0 = -3Yt^2 + t + 4t^7,$$

so, for $t \neq 0$,

$$Y = \frac{1 + 4t^6}{3t}.$$

This parametrization goes to infinity as $t \to 0$; it describes a remote branch of the bisector envelope. The local boundary near the origin is instead controlled by the limiting family of almost vertical bisectors and the tangent-cone half-plane $X \leq 0$. Thus the ramphoid cusp has a two-dimensional cell, but its local boundary has a leading straight side rather than a finite smooth caustic through the origin. This example shows that the envelope can have components at infinity or fail to be the most visible local boundary germ.

Remark 6.1. *This behavior is not a contradiction. For $\gamma(t) = (t^2, t^5)$, the leading comparison is $2Xt^2 \leq t^4$, hence $X \leq t^2/2$ for all small t, forcing the local limiting boundary $X = 0$. Higher-order terms determine how the global boundary bends away from the origin.*

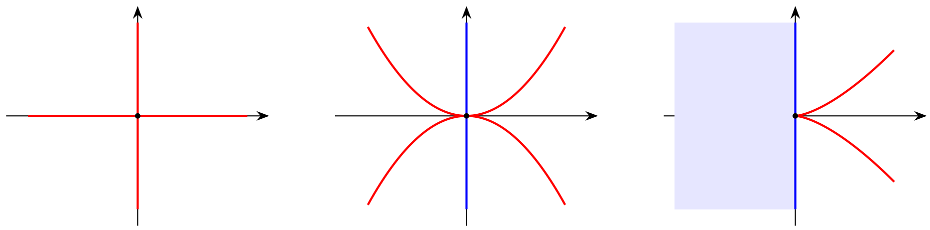

Figure 2: Semi-tangent directions distinguish nodes and tacnodes from cusps. The node and tacnode have opposite leading directions and no two-dimensional singular cell. The even cusp has a one-sided leading direction and hence a two-dimensional cell.

6.4 The ordinary node

For the node

$$C : xy = 0,$$

the real branches are the two coordinate axes. The singular point is the origin. Since each branch contains points on both sides of the origin, the semi-tangent cone contains

$$(1, 0),\ (-1, 0),\ (0, 1),\ (0, -1).$$

The polar cone is $\{0\}$. Hence the node has no two-dimensional local Voronoi cell. In fact, if the whole curve is the union of the coordinate axes, the only point closer to the origin than to all other points on the axes is the origin itself.

6.5 The tacnode

For the tacnode

$$C : y^2 = x^4,$$

the two branches are

$$\gamma_1(t) = (t, t^2), \qquad \gamma_2(t) = (t, -t^2).$$

Both branches have two-sided leading direction along the x-axis. Hence the semi-tangent cone contains $(1, 0)$ and $(-1, 0)$, so the polar cone is contained in the Y-axis. Thus the singular point has no two-dimensional Voronoi cell.

7 Relation with wave fronts and cut loci

For a curve C, the wave front at distance r is

$$W_r(C) = \{z \in \mathbb{R}^2 : \mathrm{dist}(z, C) = r\}.$$

Equivalently, it is the boundary of the offset or parallel set at distance r. For smooth curves, singularities of these fronts are governed by the evolute and by self-intersections of the normal exponential map. This is the classical setting of caustics, focal sets, medial axes and symmetry sets.

The singular Voronoi cell of $p \in \mathrm{Sing}(C)$ has a simple wave interpretation: it is the set of points reached by the wave emitted from p no later than by the waves emitted from any other point of C. Its boundary is where the wave from p and a wave from a nearby branch arrive simultaneously:

$$|z - p| = |z - \gamma(t)|.$$

Thus the singular Voronoi caustic is the caustic of a family of bisectors, rather than the ordinary caustic of the normal map.

In the smooth case the cut locus consists of points with more than one nearest point, together with focal limiting points. For singular curves it is natural to enlarge the cut locus by adding boundaries of singular Voronoi cells. This leads to the following object.

Definition 7.1. *The* singular cut locus *of a real algebraic curve C is the union, over singular points $p \in \mathrm{Sing}(C)$, of the boundaries of the full-dimensional pieces of $\mathcal{V}_C(p)$, together with their limiting focal and medial-axis endpoints.*

This terminology is provisional, but it is useful because it separates the singular contribution from the already well-studied smooth medial axis and evolute.

8 Effective construction for a singular point

Let C be given by $P(x, y) = 0$, and let $p \in C$ be a real singular point. The preceding discussion gives the following algorithmic local construction.

Step 1. Translate p to the origin.

Step 2. Compute the real Puiseux parametrizations of the local real branches.

Step 3. Extract the semi-tangent cone $\mathcal{T}_0^+ C$.

Step 4. Compute its polar cone. If the polar cone has empty interior, the singular point has no two-dimensional local Voronoi cell.

Step 5. If the polar cone has interior, form for each branch $\gamma_j(t)$ the bisector equation

$$2\langle z, \gamma_j(t)\rangle = |\gamma_j(t)|^2.$$

Step 6. Compute the envelope by adding

$$\frac{\partial}{\partial t}\left(2\langle z, \gamma_j(t)\rangle - |\gamma_j(t)|^2\right) = 0.$$

Step 7. Intersect the corresponding half-plane inequalities and retain the envelope arcs which actually occur in the boundary.

This procedure is semialgebraic and effective. It is the singular analogue of the critical-ideal construction of [7]: one keeps the equidistance equation, but replaces the smooth normal-space condition at the fixed site by the singular site itself and imposes normality only at the moving smooth point. In principle, one can eliminate the Puiseux parameter t to obtain algebraic equations for the boundary components.

9 Global Voronoi portraits

We now pass from a single point to the family of Voronoi cells of all points of a fixed real algebraic curve. For a closed real algebraic curve $C \subset \mathbb{R}^2$ and a point $z \in \mathbb{R}^2$, set

$$M_C(z) = \{p \in C : |z - p| = \mathrm{dist}(z, C)\}.$$

Thus $M_C(z)$ is the set of all nearest points of the curve to z. The global Voronoi cells are

$$\mathcal{V}_C(p) = \{z \in \mathbb{R}^2 : p \in M_C(z)\}, \qquad p \in C.$$

Since a real algebraic curve is closed, the set $M_C(z)$ is non-empty for every $z \in \mathbb{R}^2$, and therefore

$$\bigcup_{p \in C} \mathcal{V}_C(p) = \mathbb{R}^2.$$

So the informative global object is not the union itself, but the locus where the nearest-point map changes.

Definition 9.1. *The* jump locus *(or global codimension-one Voronoi skeleton) of C is*

$$J_C := \{z \in \mathbb{R}^2 : \# M_C(z) \geq 2\}.$$

Its complement $\mathbb{R}^2 \setminus J_C$ will be called the set of Voronoi chambers *of C.*

Across J_C the nearest point on the curve jumps discontinuously. On the other hand, on any chamber the nearest point is unique. This produces the natural stratification of the plane requested above.

Proposition 9.2 (Nearest-point chambers)**.** *Let U be a connected component of $\mathbb{R}^2 \setminus J_C$. Then the map*

$$\pi_C : U \to C, \qquad \pi_C(z) = \text{ the unique point of } M_C(z),$$

is well-defined and continuous. Moreover:

- (i) *if $\pi_C(U)$ is contained in the smooth locus of C and avoids focal degeneracies, then π_C is real-analytic on U and U is foliated by normal segments/rays;*
- (ii) *if $U \subset \mathcal{V}_C(s)$ for some singular point $s \in \operatorname{Sing}(C)$, then π_C is constant on U.*

Proof. Uniqueness of the nearest point on U gives a continuous nearest-point map by standard compactness arguments. In the smooth non-focal case one applies the implicit function theorem to the normal projection equations. If the unique nearest point is a fixed singular point, the map is obviously constant. □

This suggests distinguishing two related global objects:

$$\Sigma_C := \bigcup_{s \in \operatorname{Sing}(C)} \operatorname{int} \mathcal{V}_C(s),$$

which we call the *singular Voronoi domain*, and the jump locus J_C, which is the codimension-one set where the nearest point changes. The boundary of the full chamber decomposition comes from three mechanisms.

1. *Smooth–smooth competition:* two or more distinct smooth points of C are simultaneously nearest. This produces the ordinary symmetry set / medial-axis part of J_C.
2. *Singular–smooth competition:* a singular point and a smooth point are simultaneously nearest. This produces the singular bisector envelopes studied above and forms part of J_C.
3. *Focal degeneration:* the normal projection ceases to be locally regular. This is detected by the evolute. The evolute is not itself usually a jump locus, but it controls endpoints, cusps and reconnections of the branches of J_C.

In formulas, if $s \in \operatorname{Sing}(C)$ and $q \in C_{\mathrm{sm}}$ is active, then a smooth boundary point z of $\mathcal{V}_C(s)$ satisfies

$$|z - s| = |z - q|, \qquad z - q \perp T_q C.$$

Thus the boundary is the envelope of the perpendicular bisectors of the chords sq.

9.1 The normal-equidistant curve and the algebraic closure of the jump locus

Let

$$C = \{(x, y) \in \mathbb{R}^2 : E(x, y) = 0\}$$

be a real plane algebraic curve. We define the *normal-equidistant curve* of the smooth locus of C to be the Zariski closure of the set of points $z = (X, Y)$ for which there exist two distinct smooth points

$$q_i = (u_i, v_i) \in C_{\mathrm{sm}}, \qquad i = 1, 2,$$

such that both segments zq_i are normal to C and have the same length. Equivalently, z is the center of a circle tangent to C at two distinct smooth points. This is the classical *symmetry set* of Bruce–Giblin–Gibson, or the *Maxwell set* of the squared-distance family in the terminology of singularity theory.

Proposition 9.3 (Elimination equation for the algebraic closure)**.** *The algebraic closure of the smooth–smooth part of the jump locus is contained in the plane algebraic curve obtained by eliminating u_1, v_1, u_2, v_2 from the system*

$$\begin{cases} E(u_1,v_1)=0, \qquad E(u_2,v_2)=0, \\ (X-u_1)E_y(u_1,v_1)-(Y-v_1)E_x(u_1,v_1)=0, \\ (X-u_2)E_y(u_2,v_2)-(Y-v_2)E_x(u_2,v_2)=0, \\ (X-u_1)^2+(Y-v_1)^2=(X-u_2)^2+(Y-v_2)^2. \end{cases} \tag{NE}$$

Equivalently, if I is the ideal generated by these five equations and

$$D=(u_1-u_2)^2+(v_1-v_2)^2,$$

then the desired algebraic curve is defined by the elimination ideal

$$\big(I : D^\infty\big)\cap \mathbb{R}[X,Y].$$

The saturation by D removes the tautological diagonal $q_1=q_2$.

Proof. The first two equations say that q_1 and q_2 lie on C. The next two equations say that $z-q_i$ is orthogonal to the tangent line to C at q_i, equivalently parallel to the gradient $\nabla E(q_i)$. The last equation imposes equality of the two squared normal lengths. Therefore every smooth–smooth point of the jump locus satisfies (NE). Removing the diagonal and taking the Zariski closure gives exactly the stated elimination ideal. The true jump locus is obtained from the real points of this algebraic curve by imposing the additional nearest-point inequalities below. □

The real semialgebraic jump locus J_C is generally a proper subset of the real points of the normal-equidistant curve. It is selected by the global inequalities

$$|z-q_1|^2=|z-q_2|^2\le |z-q|^2 \qquad \text{for all } q\in C.$$

Thus the algebraic equation gives the symmetry/Maxwell set, whereas the actual Voronoi chamber wall is its nearest-point, or medial-axis, part.

For singular curves one must add singular–smooth components. If $s\in \mathrm{Sing}(C)$ and $q=(u,v)\in C_{\mathrm{sm}}$, the corresponding algebraic continuation is obtained from

$$\begin{cases} E(u,v)=0, \\ |z-s|^2=|z-q|^2, \\ (X-u)E_y(u,v)-(Y-v)E_x(u,v)=0. \end{cases} \tag{SE}$$

These are precisely the singular bisector envelopes constructed locally in the earlier sections. If two singular points compete, one obtains the ordinary perpendicular bisector of the two singular sites, again subject to the global nearest-point inequalities.

Remark 9.4 (Relation with the Euclidean distance discriminant)**.** *The normal-equidistant curve should not be confused with the ordinary Euclidean distance discriminant in the ED-degree sense. The latter is the caustic or branch locus of the ED correspondence; for a smooth plane curve it is essentially the evolute. By contrast, the normal-equidistant curve records two* distinct *critical points with the same critical value. In the language of singularity theory of the squared-distance family, it is the Maxwell set, whereas the evolute is the caustic. Their union is the natural bifurcation set of the nearest-point problem.*

The following examples show how the chamber picture looks globally. The examples of conics, cubics, quadrifolium and Dürer's folium are inspired by the florilegium in [11], especially Section 8.

9.2 Ellipse

For the ellipse

$$C: \quad x^2/a^2 + y^2/b^2 = 1,$$

there are no affine singularities, hence $\Sigma_C = \varnothing$. The global geometry is therefore governed by smooth normal cells and by the jump locus J_C. In this case the interior jump locus is the familiar medial-axis segment on the major axis, namely the segment between the two centers of curvature at the major-axis vertices:

$$J_C^{\mathrm{int}} = \left[-\frac{a^2-b^2}{a}, \frac{a^2-b^2}{a}\right] \times \{0\}.$$

The evolute is the astroid

$$X = \frac{a^2-b^2}{a}\cos^3 t, \qquad Y = \frac{b^2-a^2}{b}\sin^3 t.$$

The nearest-point map is single-valued on each connected component of $\mathbb{R}^2 \setminus J_C$. Inside the ellipse, the jump occurs across the green segment; outside the ellipse the nearest point is unique, although the evolute still governs the focal behavior of the normal family. The full normal-equidistant curve is larger than the medial part: for $a > b$ it consists of the horizontal segment above together with the vertical segment

$$\{0\} \times \left[-\frac{a^2-b^2}{b}, \frac{a^2-b^2}{b}\right].$$

The vertical segment corresponds to equal-length normal chords which are not globally shortest; it is part of the symmetry set but not of the jump locus.

9.3 Hyperbola

For the hyperbola

$$C: \quad x^2/a^2 - y^2/b^2 = 1,$$

there is again no singular Voronoi domain. The new feature is the coexistence of two non-compact branches. At least one prominent branch of the jump locus is forced by symmetry: the axis $x = 0$ consists of points with two symmetric nearest points, one on each branch. Thus $x = 0 \subset J_C$. In addition, the non-compactness creates a substantial global truncation phenomenon for the one-dimensional normal cells.

The evolute is the Lamé-type curve

$$X = \pm\frac{a^2+b^2}{a}\cosh^3 t, \qquad Y = \frac{a^2+b^2}{b}\sinh^3 t.$$

In this example the evolute and the jump locus should be viewed as complementary: the evolute records focal degeneration of the normal map, while the green vertical branch records genuine discontinuity of the nearest-point map.

9.4 The ordinary cusp

For

$$C: \quad y^2 + x^3 = 0, \qquad \gamma(t) = (-t^2, t^3),$$

the singular point $s = (0,0)$ has a one-sided semi-tangent cone. Hence $\operatorname{int} \mathcal{V}_C(s) \neq \varnothing$. In this example the singular Voronoi domain is already one of the Voronoi chambers, and its boundary is part of the jump locus J_C. The singular Voronoi caustic is

$$X = \frac{t^2+3t^4}{2}, \qquad Y = t + 2t^3.$$

On one side of this curve the unique nearest point is the cusp; on the other side the nearest point lies on the smooth part of the branch. Thus the envelope is simultaneously the boundary of the singular cell and a codimension-one jump curve.

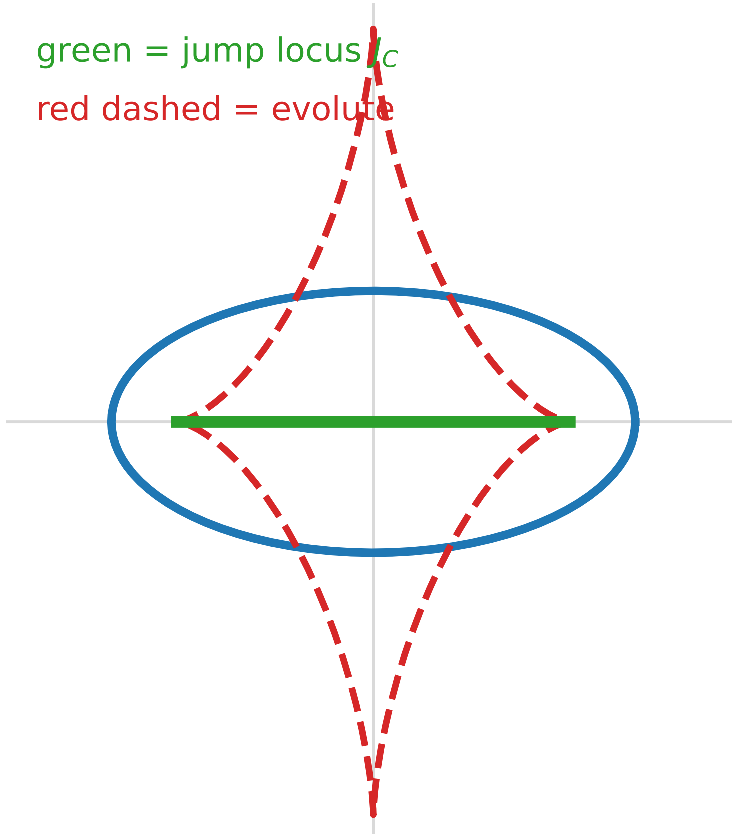

Figure 3: Ellipse: blue = the curve, red dashed = the evolute, green = the nearest-point jump locus J_C, namely the major-axis segment between the two focal endpoints.

9.5 A nodal cubic

Consider the nodal cubic

$$C: \quad 5(x^2 - y^2)(x-1) + (x^2 + y^2) = 0.$$

The origin is an ordinary real node. Its semi-tangent cone contains two opposite pairs of rays, so its polar cone is trivial. Consequently the node does *not* create a two-dimensional singular chamber:

$$\operatorname{int} \mathcal{V}_C(0) = \varnothing.$$

Nevertheless the loop of the cubic contributes a genuine one-dimensional smooth–smooth branch of the jump locus. Since the equation is even in y, the loop is symmetric with respect to the x-axis. Writing the upper half of the loop as

$$y^2 = \frac{x^2(4-5x)}{6-5x}, \qquad 0 \le x \le \frac{4}{5},$$

one checks that the center $(X, 0)$ of the normal chord joining the symmetric points $(x, \pm y)$ is given by

$$X(x) = x + y\,\frac{dy}{dx} = \frac{5x(5x-4)(2x-3)}{(6-5x)^2}.$$

Hence the smooth–smooth branch of J_C on the x-axis extends from the node to the focal endpoint $X_* = X(x_*)$, where x_* is the unique root in $(0, 4/5)$ of

$$25x^3 - 90x^2 + 108x - 36 = 0.$$

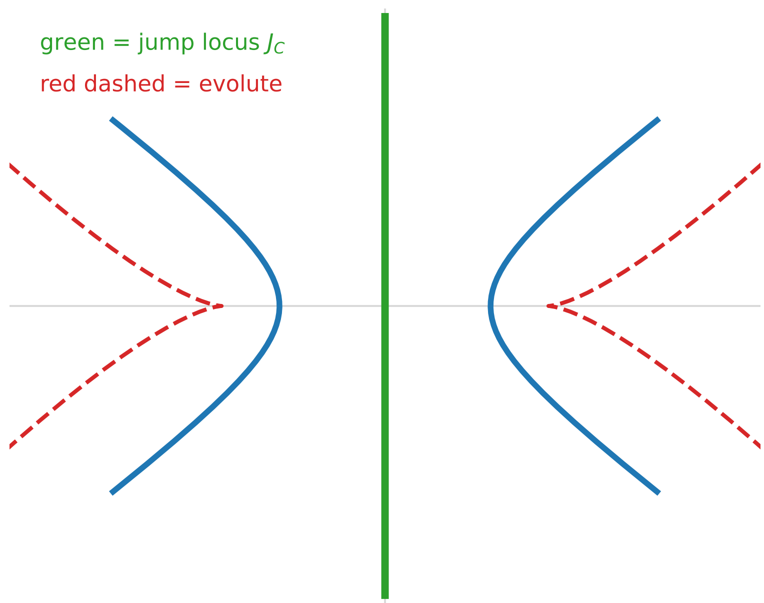

Figure 4: Hyperbola: blue = the curve, red dashed = the evolute, green = the branch $x = 0$ of the jump locus, where the two real branches compete.

Numerically,

$$x_* \approx 0.4323, \qquad X_* \approx 0.5759.$$

Thus the node contributes no open singular chamber. On the other hand, by the same symmetry argument the two unbounded real branches contribute the negative real half-axis to the jump locus, while the loop contributes the positive segment ending at X_*. The resulting visible jump locus is therefore the union of a negative half-axis and a positive segment on the real axis.

9.6 Quadrifolium and Dürer folium

The quadrifolium

$$C : \quad (x^2 + y^2)^3 - 4x^2y^2 = 0$$

has a high-multiplicity singularity at the origin, but its semi-tangent cone contains both coordinate axes. Therefore the origin contributes no open singular Voronoi chamber. Nevertheless its global symmetry set is rich. Because the curve has full dihedral symmetry, the natural candidate jump picture is given by the four symmetry lines $x = 0$, $y = 0$, $y = x$, and $y = -x$. We indicate these four lines in the left-hand panel of Figure 7.

A related rational example is Dürer's folium,

$$C : \quad (x^2 + y^2)\big(2(x^2 + y^2) - 1\big)^2 - x^2 = 0.$$

It also has pronounced symmetries and several competing loops. In this example we indicate the two symmetry axes together with two additional inner arcs, symmetric with respect to the y-axis. The arcs are drawn inside the folium, do not meet the blue curve, and schematically represent the locus equidistant from the nearest inner and outer branches. Deriving their exact equations requires a separate elimination analysis.

9.7 Local perestroikas of the jump locus

We now make the local transition picture precise. The point of the discussion is not to reprove the general singularity theory of symmetry sets, but to isolate the additional phenomena caused by singular sites. We

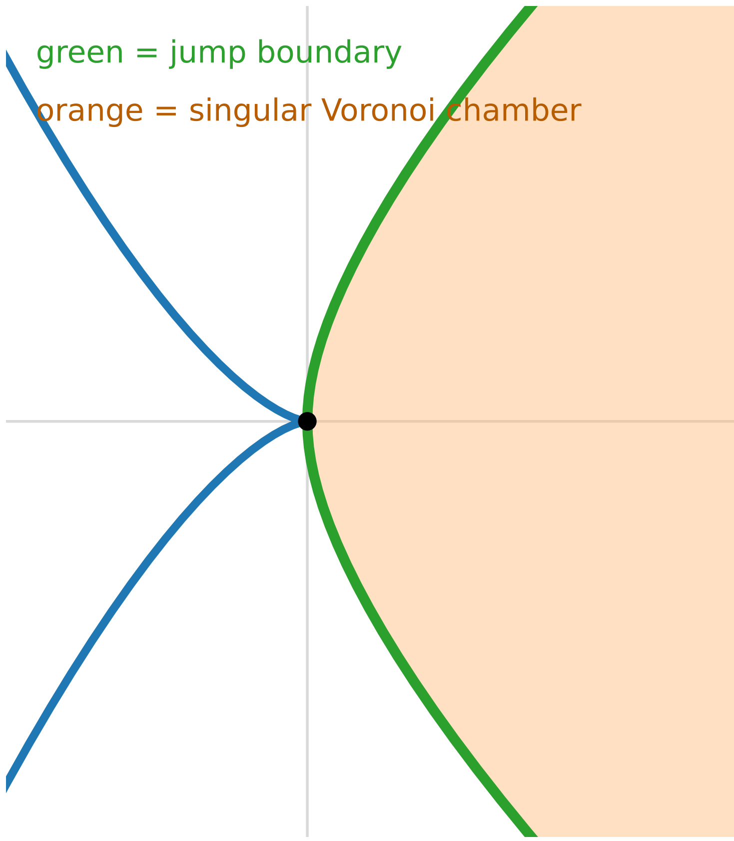

Figure 5: Ordinary cusp: orange = the two-dimensional singular Voronoi chamber, green = its jump boundary. Crossing the green curve changes the nearest point from the cusp to a smooth point of the branch.

work locally in the plane and impose explicit genericity assumptions. Under these assumptions the nearest-point stratification is reduced to a finite competition between analytic squared-distance functions.

Let $C_1, \dots, C_m$ be finitely many smooth local branches of the curve and let $s_1, \dots, s_r$ be singular points. Near a point z_0 which is not focal for the branch C_i, the squared distance to C_i is a real analytic function, denoted $\delta_i(z)$. For a singular site s_a we write

$$\delta_{s_a}(z) = |z - s_a|^2.$$

After restricting to a sufficiently small neighborhood and discarding non-active branches, the local nearest-point problem is therefore described by a finite family of real analytic functions

$$f_1(z), \dots, f_N(z).$$

The chambers are the regions where one of the f_i is strictly smaller than all the others, and the jump locus is the set where the minimum is attained at least twice.

Lemma 9.5 (Analytic competition lemma)**.** *Let $f_1, \dots, f_N$ be real analytic functions near $z_0 \in \mathbb{R}^2$, and set*

$$J = \{z : \min_i f_i(z) \text{ is attained for at least two indices}\}.$$

Assume that $f_1(z_0) = f_2(z_0) < f_j(z_0)$ for $j \geq 3$ and that

$$\nabla(f_1 - f_2)(z_0) \neq 0.$$

Then, near z_0, J is a smooth analytic arc given by $f_1 = f_2$. It separates two chambers, one where $f_1 < f_2$ and one where $f_2 < f_1$.

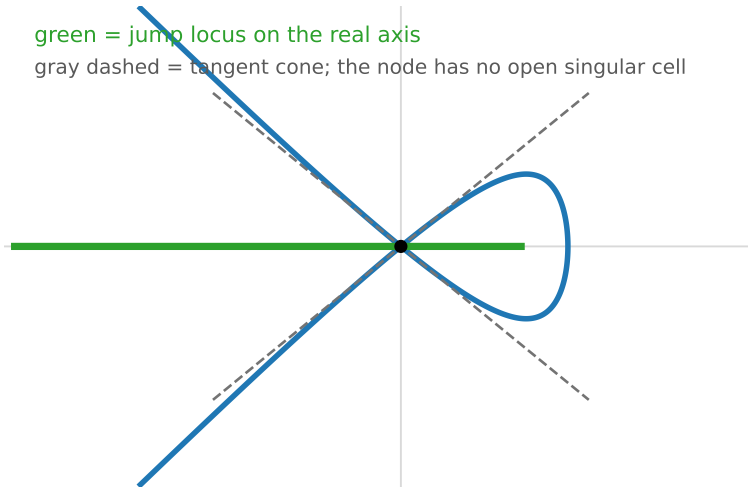

Figure 6: Nodal cubic. The dashed lines show the tangent cone at the node, explaining why the node itself has no open singular Voronoi cell. The green locus on the real axis consists of the negative half-axis together with the positive segment produced by the loop.

Proof. The inactive functions f_j, $j \geq 3$, remain larger than f_1 and f_2 after shrinking the neighborhood. By the implicit function theorem, $f_1 - f_2 = 0$ is a smooth analytic arc. Since $f_1 - f_2$ changes sign across this arc, the two sides are precisely the two local chambers. $\square$

Lemma 9.6 (Triple-point model)**.** *Assume that*

$$f_1(z_0) = f_2(z_0) = f_3(z_0) < f_j(z_0), quadj \geq 4,$$

and that the two gradients

$$\nabla(f_2 - f_1)(z_0), \qquad \nabla(f_3 - f_1)(z_0)$$

are linearly independent. Then the jump locus near z_0 is analytically equivalent to the standard three-ray tropical vertex

$$\{(u,v) : u = 0,\ v \geq 0\} \cup \{(u,v) : v = 0,\ u \geq 0\} \cup \{(u,v) : u = v \leq 0\}.$$

In particular, three chambers meet at z_0.

Proof. Set

$$u = f_2 - f_1, \qquad v = f_3 - f_1.$$

By the rank assumption, (u,v) gives local analytic coordinates. In these coordinates the three relevant functions differ from f_1 by $0, u, v$. Hence the minimum is attained twice exactly when the minimum of $0, u, v$ is attained twice. This is the standard tropical vertex displayed above. The remaining f_j are inactive after shrinking the neighborhood. $\square$

The two lemmas prove the local structure of smooth–smooth and singular–smooth jump arcs away from focal points. Indeed, if a smooth branch B has a unique non-focal closest point q to z_0, then δ_B is analytic near z_0. If a singular point s competes with B, the boundary of the singular cell is just

$$|z - s|^2 = \delta_B(z),$$

and Lemma 9.5 applies whenever the two gradients are distinct. The condition that q is the closest point on B is exactly the normality condition $z - q \perp T_q B$; eliminating q gives the singular bisector envelope discussed earlier.

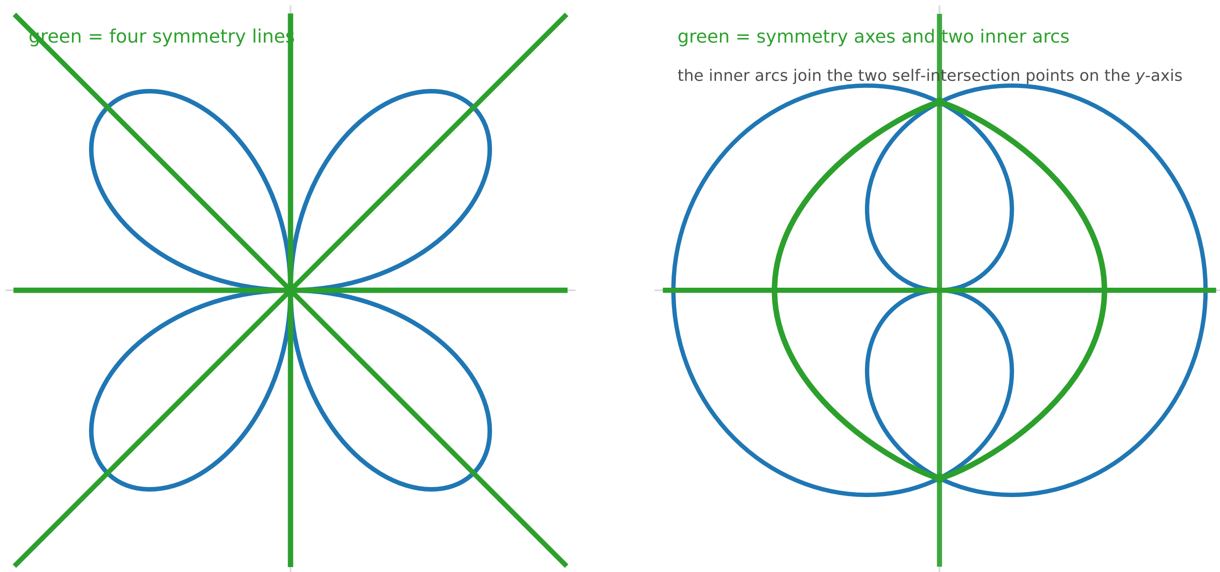

Figure 7: Two global test examples. Left: quadrifolium. The green picture shows the four symmetry lines suggested for the jump locus. Right: Dürer's folium. The green picture shows the symmetry axes together with two inner arcs, symmetric with respect to the y-axis, representing the expected equal-distance loci between the nearest inner and outer branches. The jump locus for the Dürer's folium is schematic.

Proposition 9.7 (Smooth, singular, and mixed jump arcs)**.** *Let z_0 be a point of the jump locus and suppose that all active smooth nearest points are non-focal and that at most two active sites occur. Then, under the transversality condition of Lemma 9.5, the jump locus is a smooth analytic arc near z_0. The three possible types are:*

(i) *smooth–smooth: two distinct smooth nearest points have equal distance;*

(ii) *singular–smooth: one singular point and one smooth point have equal distance;*

(iii) *singular–singular: two singular points have equal distance, giving a piece of their ordinary perpendicular bisector.*

In each case the arc separates the two corresponding nearest-point chambers.

Proof. For smooth active points, non-focality gives analytic squared-distance functions by the implicit function theorem applied to the normality equations. For singular points the squared-distance functions are simply quadratic polynomials. Thus the problem is a finite analytic competition. Lemma 9.5 gives the conclusion. In the singular–singular case the equality $|z-s_1|^2 = |z-s_2|^2$ is the usual perpendicular bisector. □

Proposition 9.8 (Triple reconnection)**.** *Suppose that exactly three active non-focal sites, smooth or singular, are nearest to z_0, and that the gradients of two independent differences of the corresponding squared-distance functions are linearly independent. Then the local jump locus is a three-ray vertex as in Lemma 9.6. This is the elementary reconnection perestroika of the nearest-point chamber decomposition.*

Proof. This is precisely Lemma 9.6, with the inactive branches removed by shrinking the neighborhood. □

Next we record the precise role of the evolute. It is not usually a jump locus by itself. Rather, it is the caustic of the smooth normal projection and marks where the analytic distance-to-a-branch function ceases to be regular.

Proposition 9.9 (Focal transition)**.** *Let B be a smooth branch parametrized by arclength $\gamma(s)$, with unit normal $n(s)$ and signed curvature $\kappa(s)$. The normal map*

$$\Phi(s,r) = \gamma(s) + rn(s)$$

has Jacobian

$$\det D\Phi(s,r) = 1 - r\kappa(s).$$

Consequently the focal locus of B is the evolute

$$\gamma(s) + \frac{1}{\kappa(s)} n(s),$$

at points where $\kappa(s) \neq 0$. Away from this locus the squared distance to B is analytic; at this locus the normal parametrization loses local invertibility, and endpoints or cusps of branches of the jump locus can occur only through the usual caustic mechanism or through simultaneous competition with another active site.

Proof. Since $\gamma'(s) = T(s)$ and $n'(s) = -\kappa(s)T(s)$, one has

$$\partial_s \Phi = (1 - r\kappa(s))T(s), \qquad \partial_r \Phi = n(s).$$

Thus the Jacobian determinant in the oriented frame (T, n) is $1 - r\kappa(s)$. The critical values are therefore exactly the centers of curvature. The final assertion follows from the implicit function theorem away from the critical values. □

We now state the singular perestroika which is specific to the present paper. It follows directly from the semi-tangent cone theorem, but it is useful to have an explicit normal form.

Proposition 9.10 (Singular-sector transition)**.** *Consider the one-parameter family of real curve germs*

$$C_\tau : \quad y^2 = x^2(x + \tau)$$

at the origin. Then:

(i) *for $\tau > 0$, the origin is an ordinary real node and the polar of the semi-tangent cone is $\{0\}$; hence the origin has no two-dimensional local Voronoi cell;*

(ii) *for $\tau = 0$, the origin is an ordinary cusp $y^2 = x^3$, the semi-tangent cone is the ray $\mathbb{R}_{\geq 0}(1,0)$, and the polar cone is the half-plane $\{X \leq 0\}$; hence a two-dimensional singular Voronoi sector appears;*

(iii) *for $\tau < 0$, the origin is an isolated real point of the germ and its local Voronoi cell contains a full neighborhood of the origin.*

Thus the birth of a singular Voronoi chamber is governed by the change of the polar of the real semi-tangent cone.

Proof. For $\tau > 0$, the lowest homogeneous part of the equation is $y^2 - \tau x^2$, giving two transverse real tangent lines. Each line contributes both oriented semi-tangent directions, so the polar cone is trivial. Theorem 3.2 gives no two-dimensional local cell.

For $\tau = 0$, the real cusp is parametrized by $x = t^2$, $y = t^3$. Both sides of the parametrization have the same leading vector $(1, 0)$. Hence the semi-tangent cone is the ray $\mathbb{R}_{\geq 0}(1, 0)$ and its polar is the half-plane $X \leq 0$. Theorem 3.2 gives a two-dimensional local cell.

For $\tau < 0$, if $|x|$ is sufficiently small and $x \neq 0$, then $x + \tau < 0$, so $x^2(x + \tau) < 0$ and the equation has no real solutions except $(0, 0)$. Thus the origin is an isolated real point of the germ, and sufficiently small points of the plane are closer to it than to any other point of the local germ. □

Finally, mixed singular–smooth attachments are again finite analytic competitions.

Proposition 9.11 (Attachment of a singular envelope)**.** *Suppose that at z_0 a singular site s and two non-focal smooth nearest points q_1, q_2 are all active, and that the two gradients*

$$\nabla(\delta_{q_1} - \delta_s)(z_0), \qquad \nabla(\delta_{q_2} - \delta_s)(z_0)$$

are linearly independent, where δ_{q_i} denotes the local squared-distance function to the corresponding smooth branch. Then the local jump locus is a three-ray vertex. One ray is smooth–smooth, and the other two are singular–smooth. This is the generic attachment of a singular envelope to the ordinary smooth jump locus.

Proof. Apply Lemma 9.6 to the three analytic functions δ_s, δ_{q_1} and δ_{q_2}. □

Combining these statements gives the following local classification under the stated non-focality and transversality hypotheses.

Theorem 9.12 (Local nearest-point perestroikas)**.** *For a generic local one-parameter family of real plane curve germs, assume that at the critical parameter exactly one elementary degeneracy occurs and that no four active sites have equal distance. Then the local changes of the nearest-point chamber decomposition are generated by:*

(i) *birth, death, or smooth passage of a two-site jump arc, as in Proposition 9.7;*

(ii) *triple reconnection of three chambers, as in Proposition 9.8;*

(iii) *focal transition of a smooth branch at the evolute, as in Proposition 9.9;*

(iv) *birth or disappearance of a singular chamber through a change of the semi-tangent cone, with model Proposition 9.10;*

(v) *attachment of a singular–smooth envelope to the ordinary smooth jump locus, as in Proposition 9.11.*

In particular, the new transitions not present in the purely smooth theory are exactly those involving the polar of the semi-tangent cone of a singular site.

Proof. Away from focal points and singularities, the nearest-point problem reduces to a finite collection of analytic squared-distance functions. If two functions are active, Lemma 9.5 applies; if three are active, Lemma 9.6 applies. The exclusion of four equal active values and the transversality assumptions rule out higher multiple vertices and non-transverse tangencies. If a smooth active point is focal, Proposition 9.9 gives the only possible loss of regularity of the smooth distance function. If the active site is singular, Theorem 3.2 reduces the local birth of a two-dimensional singular chamber to the appearance of a non-empty polar sector of the semi-tangent cone, and Proposition 9.10 gives the basic model. Finally, if a singular site and two smooth sites are simultaneously active, Proposition 9.11 gives the generic attachment. These alternatives exhaust the allowed elementary degeneracies. □

These results explain why the evolute and the jump locus should be studied together. The evolute controls the focal singularities of the smooth normal family, while the jump locus records the actual discontinuities of the nearest-point map. Singular Voronoi cells supply an additional mechanism not present in the purely smooth theory.

Remark 9.13 (Effective global plotting strategy)**.** *For a fixed algebraic curve $P(x, y) = 0$, a practical global plot can be assembled in the following order.*

(1) *Compute the singular Voronoi chambers using the semi-tangent cone criterion and the singular bisector-envelope equations.*

(2) *Compute the smooth–smooth jump locus by solving for pairs of smooth points $q_1, q_2 \in C$ such that*

$$\begin{cases} P(q_1) = P(q_2) = 0, \;\; q_1 \neq q_2, \\ z - q_i \perp T_{q_i} C, \\ |z - q_1| = |z - q_2|. \end{cases}$$

(3) *Compute the evolute in order to locate focal endpoints, cusps and other perestroikas of the jump set.*

(4) *Finally, retain only those real branches which satisfy the nearest-point inequalities and therefore truly bound Voronoi chambers.*

This is the global counterpart of the local constructions developed in the earlier sections.

10 Additional results

10.1 The simple singularities of type A_k

The real forms of the plane curve singularity of type A_k may be written, after a local analytic change of coordinates, as

$$y^2 - x^{k+1} = 0 \qquad \text{or} \qquad y^2 + x^{k+1} = 0.$$

The semi-tangent criterion gives a complete first-order answer for this series.

Proposition 10.1 (The A_k-series)**.** *Let $(C, 0)$ be a real plane curve singularity of type A_k.*

(i) *If k is even, then each real form has a cuspidal real branch. The leading parametrized term has even order, and the singular point has a two-dimensional local Voronoi cell.*

(ii) *If k is odd and the real form is $y^2 - x^{k+1} = 0$, then the germ consists of two real branches with opposite semi-tangent directions. The singular point has no two-dimensional local Voronoi cell.*

(iii) *If k is odd and the real form is $y^2 + x^{k+1} = 0$, then the origin is an isolated real point. Its local Voronoi cell contains a full neighborhood of the origin.*

Proof. If k is even, then $k+1$ is odd. The real branches of $y^2 = \pm x^{k+1}$ are cuspidal and can be parametrized as

$$x = \pm t^2, \qquad y = t^{k+1}.$$

The first non-zero vector is one-sided, namely $(\pm 1, 0)$, and therefore the polar of the semi-tangent cone contains a half-plane. Theorem 3.2 gives a two-dimensional cell.

If k is odd, then $k+1$ is even. The form $y^2 - x^{k+1} = 0$ has two real branches

$$y = \pm x^{(k+1)/2},$$

which are two-sided in the x-direction. Hence both $(1, 0)$ and $(-1, 0)$ occur in the semi-tangent cone, and the polar has empty interior. The form $y^2 + x^{k+1} = 0$ has no real points near the origin except the origin itself, so Proposition 4.7 applies. ☐

Remark 10.2. *Thus the existence of a two-dimensional singular Voronoi cell is not determined by the complex analytic type alone. For A_{2r+1} the two real forms behave differently: one gives a tacnode-type two-sided real germ and the other gives an isolated real point.*

10.2 Monomial cusps and the degree of the caustic

The bisector-envelope construction is especially transparent for monomial branches. Consider a real branch

$$\gamma(t) = (-t^m, t^n), \qquad 2 \le m < n,$$

with m even, so that the leading direction is one-sided. Put $r = n - m$. The bisector inequality is

$$X \ge Yt^r - \frac{t^m + t^{2n-m}}{2}.$$

The envelope is obtained from

$$X = Yt^r - \frac{t^m + t^{2n-m}}{2}, \qquad 0 = rYt^{r-1} - \frac{m}{2}t^{m-1} - \frac{2n-m}{2}t^{2n-m-1}.$$

When $n < 2m$, this gives the polynomial parametrization

$$\boxed{Y = \frac{m}{2(n-m)} t^{2m-n} + \frac{2n-m}{2(n-m)} t^{n},}$$

$$\boxed{X = \frac{2m-n}{2(n-m)} t^{m} + \frac{n}{2(n-m)} t^{2n-m}.}$$

Consequently the singular caustic is a rational algebraic curve of degree at most $2n - m$; for a generic such parametrization, and in particular for the higher cusps $\gamma(t) = (-t^{2k}, t^{2k+1})$, this upper bound is the actual degree.

For $\gamma(t) = (-t^{2k}, t^{2k+1})$ one recovers

$$X = \frac{2k-1}{2} t^{2k} + \frac{2k+1}{2} t^{2k+2}, \qquad Y = kt^{2k-1} + (k+1)t^{2k+1},$$

and the expected degree is $2k + 2$. The ordinary cusp therefore gives a quartic singular caustic.

If $n \geq 2m$, the displayed formula for Y has a non-positive exponent. This is exactly the phenomenon seen in the ramphoid cusp: the bisector envelope either has a component at infinity or does not give the local finite boundary through the origin. In that case the leading local boundary is the straight side supplied by the polar cone, and higher terms determine how the global boundary bends away from the singular point.

10.3 A global truncation criterion

Let the singular point be the origin, and let w be a direction in the interior of the polar cone $(\mathcal{T}_0^+ C)^\circ$. Along the ray $z = sw$, the global inequalities are

$$2s\langle w, q\rangle \leq |q|^2, \qquad q \in C.$$

Hence the maximal length of the global cell in the direction w is

$$\rho(w) = \inf_{\substack{q \in C \\ \langle w,q\rangle > 0}} \frac{|q|^2}{2\langle w, q\rangle},$$

with the convention that $\rho(w) = +\infty$ if the set of q with $\langle w, q\rangle > 0$ is empty. Therefore the part of the global cell lying in the interior of the polar sector has the radial description

$$\boxed{\{sw : \ w \in \operatorname{int}((\mathcal{T}_0^+ C)^\circ), \ 0 \leq s \leq \rho(w)\}.}$$

This formula makes precise how the rest of the curve truncates the local sector. The endpoint in the direction w is caused by a point $q \in C$ at which the above infimum is attained. If the infimum is not attained, the endpoint is caused by a limiting point at infinity or by a limiting branch of the real curve.

Proposition 10.3 (Survival of the local sector)**.** *Suppose that no other real branch of C accumulates at the singular point 0. If $w \in \operatorname{int}((\mathcal{T}_0^+ C)^\circ)$, then $\rho(w) > 0$. Hence every strictly admissible singular direction survives as a non-trivial segment of the global Voronoi cell.*

Proof. The local inequalities hold for all sufficiently small $s > 0$ by Theorem 3.2. Points of the curve outside a sufficiently small neighborhood of the origin have distance bounded below by a positive constant, and therefore their inequalities are also satisfied for all sufficiently small s. Thus the admissible ray contains a non-trivial initial segment. $\square$

10.4 Meeting the medial axis and the evolute

A smooth boundary point of a singular Voronoi cell has an active smooth point $q \in C$ satisfying

$$|z| = |z - q|.$$

If q moves smoothly along a branch and gives an envelope point, then differentiating the equality gives

$$z - q \perp T_q C.$$

Thus z lies simultaneously on the perpendicular bisector of 0 and q, and on the normal line to the smooth branch at q. In other words, the singular caustic is a component of the symmetry set involving one fixed singular point and one moving smooth point.

The possible junctions with the ordinary medial axis are therefore of three elementary types:

(a) a second smooth point $q_2 \in C$ becomes active, so z has at least three nearest sites: the singular point and two smooth points;

(b) the active smooth point reaches a focal degeneracy, so the bisector-envelope point meets the ordinary evolute;

(c) a boundary ray of the polar cone is reached, corresponding to a change of the leading semi-tangent constraint.

This gives a concrete local dictionary between singular Voronoi caustics, the ordinary symmetry set, and the ordinary evolute.

10.5 Higher-dimensional analogue

The cone criterion is not special to plane curves. Let $(X, 0) \subset (\mathbb{R}^N, 0)$ be a real semialgebraic or real analytic germ, and define the semi-tangent cone $\mathcal{T}_0^+ X$ exactly as before, using leading vectors of real analytic arcs. Then the same half-space argument proves

$$T_0 \mathcal{V}_X(0) \subset (\mathcal{T}_0^+ X)^\circ,$$

and every ray in the interior of $(\mathcal{T}_0^+ X)^\circ$ belongs to the tangent cone of the local Voronoi cell. Thus the local Voronoi cell has full dimension in $\mathbb{R}^N$ exactly when the semi-tangent cone is contained in a proper closed half-space, or equivalently when its polar has non-empty interior.

For hypersurfaces this says that a smooth point again gives only the normal line, while a one-sided singularity may produce a full-dimensional solid angle. The boundary caustics are higher-dimensional envelopes of bisector hyperplanes between the singular point and nearby smooth points of the hypersurface.

11 Conclusion

The Voronoi cell of a smooth point of a plane curve is essentially a normal-line object. Singular points create a different phenomenon: a Voronoi cell may have non-empty interior. The global discussion above separates the full nearest–point stratification from the special two-dimensional cells attached to singular points and identifies the normal-equidistant curve with the classical symmetry/Maxwell set. The additional results above show that this phenomenon is already strong enough to classify the A_k-series by real form, to compute a useful degree bound for monomial cusps, and to describe global truncation by a radial support function. The local existence of such a cell is governed by the polar cone of the real semi-tangent cone. Once the cell exists, its boundary is obtained from the envelope of perpendicular bisectors between the singular point and nearby smooth branches. This gives an effective construction and a natural bridge between algebraic Voronoi theory, medial axes, wave fronts and singularity theory.

The main point is not to replace the algebraic Voronoi theory of [7] or the plane-curve medial-axis/evolute theory of [4], but to add the missing local singular contribution. The cusp example shows the phenomenon in its simplest form; nodes and tacnodes show why not every singularity contributes a two-dimensional cell; higher cusps and isolated real points show that several distinct local behaviors are possible.

Acknowledgements. The author wants to thank Kathlén Kohn who introduced me to this topic on her lecture on algebraic theory of neural networks in May 2026.

References

[1] V. I. Arnold, *Singularities of Caustics and Wave Fronts*, Mathematics and its Applications, vol. 62, Kluwer Academic Publishers, Dordrecht, 1990.

[2] V. I. Arnold, *Topological Invariants of Plane Curves and Caustics*, University Lecture Series, vol. 5, American Mathematical Society, Providence, RI, 1994.

[3] H. Blum, A transformation for extracting new descriptors of shape, in *Models for the Perception of Speech and Visual Form*, ed. W. Wathen-Dunn, MIT Press, Cambridge, MA, 1967, pp. 362–380.

[4] M. Brandt and M. Weinstein, Voronoi cells in metric algebraic geometry of plane curves, *arXiv:1906.11337*, 2019.

[5] J. W. Bruce, P. J. Giblin and C. G. Gibson, Symmetry sets, *Proceedings of the Royal Society of Edinburgh Section A* **101** (1985), 163–186.

[6] J. W. Bruce and P. J. Giblin, *Curves and Singularities*, 2nd edition, Cambridge University Press, Cambridge, 1992.

[7] D. Cifuentes, K. Ranestad, B. Sturmfels and M. Weinstein, Voronoi cells of varieties, *Foundations of Computational Mathematics* **22** (2022), 1369–1396; preprint *arXiv:1811.08395.*

[8] J. Damon and P. J. Giblin, Local features in natural images via singularity theory, *Journal of Mathematical Imaging and Vision* **21** (2004), 107–143.

[9] H. Federer, Curvature measures, *Transactions of the American Mathematical Society* **93** (1959), 418–491.

[10] P. J. Giblin and B. B. Kimia, A formal classification of 3D medial axis points and their local geometry, *IEEE Transactions on Pattern Analysis and Machine Intelligence* **26** (2004), 238–251.

[11] R. Piene, C. Riener and B. Shapiro, Return of the plane evolute, *Annales de l'Institut Fourier*, to appear; online first, 2025.

[12] J. N. Mather, Distance from a submanifold in Euclidean space, in *Singularities, Part 2*, Proceedings of Symposia in Pure Mathematics, vol. 40, American Mathematical Society, Providence, RI, 1983, pp. 199–216.